Available online at www.sciencedirect.com
SCIENCE DIRECT®
International Journal of Pharmaceutics 250 (2003) 385–401
international journal of pharmaceutics
www.elsevier.com/locate/ijpharm

Evaluation of solid dispersion particles prepared with SEDS

Anne Mari Juppo *, Catherine Boissier, Cynthia Khoo

AstraZeneca R&D Mölndal, S-431 83 Mölndal, Sweden

Received 10 April 2002; received in revised form 7 October 2002; accepted 8 October 2002

Abstract

Formation of solid solution particles in the Solution Enhanced Dispersion by Supercritical fluids (SEDS) process from a model drug and two different types of carriers, mannitol and Eudragit® E100 was evaluated. The crystal properties of samples and molecular interactions were investigated with DSC and FTIR, respectively. The effect of co-crystallisation of drug and mannitol on dissolution rate was studied. Even if a true one-phase solid dispersion was not obtained, the crystal structure of both drug and mannitol was mutually affected by the presence of the other. The drug was not in highly crystalline form in the co-precipitates. The interactions between the drug and mannitol could also be identified as hydrogen bonding between the amine or hydroxyl groups of the drug and the hydroxyl groups of mannitol. These interactions and changes in the crystal structure are probably directly related to the increase in the dissolution rate observed. A true solid solution was obtained when the drug was co-processed with Eudragit® E100. A clear interaction between the acid hydroxyl group of the drug and the basic carbonyl group on the Eudragit® E100 was observed. SEDS was shown to be an effective process for forming intimate blends and solid solutions for the drug and two different types of carriers.

Keywords: Solid dispersion; Supercritical fluid crystallisation; Particle; DSC; FTIR; SEDS

1. Introduction

Supercritical precipitation or crystallisation of drug and incorporation of drugs in a carrier by using supercritical fluids has lately become of interest. In this process, supercritical fluid is used as a dissolution media or as an anti-solvent. A material is in supercritical phase when its pressure and temperature are greater than its critical pressure and temperature. Several research groups have presented their techniques or methods for using supercritical fluid in particle preparation. The use of supercritical fluids and their properties have been reviewed for example by Tom and Debenedetti (1991). Supercritical fluid can be used as a solvent for the drug and possible excipients, and the particles are created when the supercritical fluid containing the dissolved substances is expanded in a lower temperature and pressure (Krukonis, 1994; Matson et al., 1986). This method is known as Rapid Expansion of Supercritical Solutions (RESS).

* Corresponding author. Tel.: +46-31-776-2963; fax: +46-31-776-3729
E-mail address: anne.juppo@astrazeneca.com (A.M. Juppo).

0378-5173/02/$ - see front matter
PII: S0378-5173(02)00577-X

Another way to utilise supercritical fluid is to use it as an anti-solvent for the precipitation of substances dissolved in suitable organic solvents. Compressed gases or supercritical fluids has been used as an anti-solvent in different ways (Schmitt, 1990; Müller and Fischer, 1989; Tom et al., 1993; Dixon et al., 1993; Yeo et al., 1994) but the principle for particle formulation is the same. Hanna and York (1993) presented a technique with which they claim to have a better control of size distribution of particles prepared than with the other antisolvent techniques. Here, the formation of the droplet of solution in the supercritical medium is controlled by the specific nozzle design and the parallel flow of supercritical medium with the solution in coaxial passages and the mixing of solution and supercritical fluid in the nozzle prior to the outlet end of the nozzle. The particle size can be controlled by the flow rates of the vehicle containing the solute and the flow rate of the supercritical fluid. This technique is called solution enhanced dispersion by supercritical fluids (SEDS).

Solid dispersions are generally used to enhance the dissolution of poorly water soluble drugs. The term solid dispersion includes a wide range of systems (Chiou and Riegelman, 1971). Solid dispersions can increase dissolution rate through following mechanisms; eutectic formation, increased surface area of the drug due to precipitation in the carrier, formation of true solid solution, improved wettability due to intimate contact with a hydrophilic carrier, precipitation as a metastable crystalline form or a decrease in substance crystallinity. Both the carrier–drug combination and the method of manufacture have great impact on the type of solid dispersion formed (Serajuddin, 1999).

The supercritical fluid anti-solvent technique has been tested for the preparation of solid dispersion particles for nifedipine/polyethylene glycol 4000 (Senčar-Božič et al., 1997). Ye (2000) has reported an increased release rate for lidocaine-polyethylene glycol 8000 and lidocaine-ropivacaine solid dispersions prepared with the RESS technique. This technique has also been used to precipitate homogeneous anthracene–phenanthrene crystals of solid solution (Liu and Nagahama, 1997). York et al. (2001) have produced solid solutions with the SEDS technique from several drugs using hydroxypropylmethylcellulose, hydroxypropylcellulose, ethylcellulose and polyvinylpyrrolidone as carriers. However, no pharmaceutical solid dispersions have previously been reported to be produced from other types of carriers like carbohydrates, sugar alcohols or acrylates and their derivatives using supercritical fluid processing.

The aim of this work was to investigate the possibility to prepare a solid dispersion from a model drug with two different types of carriers using the SEDS technique. The solid state and molecular interactions were evaluated.

2. Materials and methods

2.1. Materials

The model drug was 2,6-dimethyl-8-(2-ethyl-6-methylbenzylamino)-3-hydroxymethylimidazo-[1,2-a]pyridine mesylate (AstraZeneca R&D Mölndal, Mölndal, Sweden, Fig. 1). Mannitol was supplied by Roquette (Frères, France) and Eudragit® E100 (Mw 120 000 g/mol) by Röhm Pharma (Darmstadt, Germany). Acetone (99.5%), methanol (99.8%) and dimethyl sulfoxide (DMSO, 99.5%), were all supplied by Merck (Darmstadt, Germany), were used as solvents. Carbon dioxide was used as the supercritical fluid (food grade, AGA gas AB, Mölndal, Sweden).

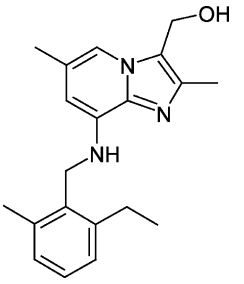

Fig. 1. Molecular structure of the model drug. Mesylate salt of this molecule was used.

2.2. Methods

2.2.1. Preparation of particles

Particles were prepared in a SEDS equipment (Bradford Particle Design, Bradford, UK) from a solution containing the drug and the carrier. The solution and the antisolvent (carbon dioxide) were introduced in a coaxial nozzle, which was located inside a pressure vessel. Under controlled pressure and temperature conditions the antisolvent extracts the solvent from the solution. The concentration of drug and carrier in the droplets increases, leading to rapid particle formation. The produced particles were collected in a vessel, while the antisolvent and the extracted solvent emerged through a back pressure regulator. The nozzle used was a two-component nozzle with an opening of 0.2 mm in diameter. In the two-component nozzle, the stream of supercritical fluid passes through the inner passage and the solution through the outer passage. The running parameters were chosen based on the optimum processing conditions for both the drug and the carrier. The parameters chosen are presented in Table 1.

The drug–carrier ratios used for preparing the particles are presented in Table 2. Control experiments were made in which pure carrier and drug were processed under the same conditions as the drug–carrier mixtures. The particles were dried in a vacuum oven at 5 mbar, 30 °C for 19 h (Vacutherm, Heraeus Instruments, Germany) before analysis in order to remove any remaining organic solvents.

2.2.2. Preparation of physical mixture

For comparison, a physical mixture of drug and mannitol was made in the ratio 64:36. The mixture was prepared by mixing in a mortar and sieving with 100 μm sieve.

2.2.3. Differential scanning calorimetry (DSC)

DSC measurements were carried out using a Perkin–Elmer, Pyris 1DSC instrument (Norwalk, USA). Approximately 5 mg of sample was analysed at a heating rate of 5 °C/min from 50 to 250 °C (or 230 °C). After cooling to 20 °C, the sample was reheated to 250 °C (or 230 °C) at the same heating rate as used in the first cycle. The analyses were made in duplicate ($n = 2$) in vented aluminium pans, under nitrogen purge. Indium was used to calibrate enthalpy and temperature.

2.2.4. Fourier transform infrared spectroscopy (FTIR)

A Perkin–Elmer FTS-1710 FTIR spectrometer (Beaconsfield, UK) equipped with a DTGS detector was used for the infrared analysis. The samples were examined in the transmission mode, as KBr pellets. A resolution of 4 per cm was used, between 25 and 30 scans were coadded for each spectrum, over a frequency range 4000–450 per cm. The software used for the data analysis was GRAMS/32 Version 5 (Galactic Industries Corporation, Salem, NH, USA).

2.2.5. Energy dispersive spectroscopy (EDS)

The instrument used was a scanning electron microscope (Jeol 840A, Tokyo, Japan) equipped with an EDS facility (Noran 5500, Thermo Noran, Middleton, WI, USA) for elemental characterisation. The EDS analysis was performed at 7 kV excitation voltage with an ultrathin window, enabling detection down to element no. 6 (i.e. carbon).

2.2.6. Scanning electron microscopy (SEM)

The particle size and morphology of the produced material were studied with a scanning electron microscopy (Jeol JSM-5400, Tokyo, Japan).

2.2.7. Drug content analysis

The true drug content in the processed samples was determined by HPLC. An isocratic chromatographic system was used (40% acetonitrile in phosphate buffer pH 3.0, $I = 0.05$). A sample of approximately 2 mg was dissolved in 25 ml mobile phase. This sample solution was further diluted five times with mobile phase. The UV–VIS detector was Spectra-Physics (Mountain View, CA, USA), Spectra 100 (wave length 248 nm). The HPLC pump and the injector used were LKB 2150 (Uppsala, Sweden) and Waters 717 with Autosampler (Waters Corp., Milford, MA, USA), respectively. The lengths of the column and the guard column (Waters Symmetri C8 5 μm)

Table 1
Processing conditions of drug–mannitol and drug–Eudragit® E100 mixtures in lab-scale SEDS process

Mixture	Solvent	Total concentration (w/v%)	Pressure (bar)	Temperature (°C)	CO_2 flow rate (ml/min)	Solution flow rate (ml/min)
Drug–mannitol	20% DMSO, 80% methanol	0.7	180	40	14	0.2
Drug–Eudragit test B1	30% DMSO, 70% acetone	7	80	35	10	0.2
Drug–Eudragit test B2	30% DMSO, 70% acetone	9	80	35	14	0.1
Drug–Eudragit test B3	30% DMSO, 70% acetone	19	80	35	14	0.1

were 150 and 20 mm, respectively. The inner diameter of both columns was 3.9 mm. The flow rate of mobile phase was 1 ml/min. The chromatographic data system was Waters Millenium 32 (Version 3.05.01).

2.2.8. Dissolution rate

The dissolution rate of the processed samples was determined using USP 4 (flow cell, CE70) technique ($n = 2$). The dissolution medium was citrate buffer solution (pH 5.0, $I = 0.05$, 37 °C). A tablet cell 12 mm in diameter was used. One rubin sphere (5 mm in size) was placed in the bottom of the flow cell. The cell was filled with 1.5 ml glass spheres about 1 mm in size before adding the sample of approximately 2 mg. The flow rate of the dissolution medium was 16 ml/min. Samples were collected every third minute for the first 15 min and thereafter, every fifth minute during the remaining 15 min. The fractions were filtered (Whatman GF/F 0.7 μm, Kent, UK) and the concentrations of the diluted samples were determined using the same HPLC method as for drug content analysis.

3. Results and discussion

3.1. Appearance of particles

The SEM graphs of pure mannitol and drug processed using the same SEDS conditions as for the drug–mannitol mixtures are presented in Fig. 2. Mannitol precipitates as long fibrous-like particles whereas the SEDS processed drug is crystallised as irregular and flaky particles (size range ca. 1–20 μm). After co-precipitation in the SEDS process, mannitol and drug particles can still be identified by their appearance (Fig. 3). Thus, no true one-phase solid dispersion with the mixtures used was obtained. Mannitol tends still to hold its crystal shape but the drug particles are less flaky (size range ca. 5–10 μm). It is possible that this reflects the effect of mannitol on the crystal structure of the drug. The EDS analysis of the two different shapes of particles confirmed that the fibrous particles only consisted of mannitol.

Table 2
Yields and drug contents of SEDS processed samples

Batch	Nominal content (%drug:%carrier)	Real content (%drug:%carrier)	Yield (%)
A1	90:10	72:28	72
A2	80:20	78:22	72
A3	70:30	64:36	84
A4	60:40	57:43	80
A5	50:50	40:60	72
A6	40:60	35:65	78
A7	30:70	24:76	84
A8	20:80	14:86	35
A9	10:90	5:95	81
B1	5:95	2:98	21
B2	15:85	11:89	3–8
B3	20:80	12:88	2–3
Drug	100:0	100:0	48[a], 21[b]
Mannitol	0:100	0:100	100
Eudragit	0:100	0:100	40

A, mannitol as carrier, B, Eudragit® E100 as carrier.
[a] In process conditions for drug–mannitol.
[b] In process conditions for drug–Eudragit® E100.

The pure Eudragit® E100 polymer, due to its low Tg (50 °C according to Bauer et al., 1998), does not form any well-defined particles in SEDS as can be expected (Fig. 4a). It has been shown that Tg of polymers can be decreased further by supercritical carbon dioxide (Shieh et al., 1996). The drug particles formed are irregular and flaky in shape even in these processing conditions (Fig. 4b). The appearance of drug–Eudragit® E100 mixture particles resembles the pure polymer particles (Fig. 5) which indicates that a solid dispersion has been formed.

3.2. Drug content and yields

When mannitol was used as a carrier, the experiments resulted in relatively high yields (Table 2). The reason could be that mannitol, as a hydrophilic material, has no tendency to dissolve into the supercritical fluid, whereas the drug is more hydrophobic and partly dissolves into the supercritical fluid and exits the pressure vessel. This can also be concluded from the observation that the drug content values of produced particles were lower than theoretical ones (Table 2).

Due to the optimisation of processing conditions for the mixtures of drug and the carrier, the yields for drug–Eudragit® E100 particles were extremely low. In the drug–mannitol particles, the true drug content was lower than the nominal values.

3.3. Differential scanning calorimetry

3.3.1. Mannitol and drug

Fig. 6a shows the change in the thermogram of pure mannitol after processing with SEDS. Melting point has decreased from 168.2 to 167.3 °C and the melting enthalpy has decreased from 286.9 to 278.9 J/g. This could be due to the decrease in crystallinity or partial change in crystal form. According to the supplier, the original polymorph of mannitol is β-mannitol which is known to be the most stable form. Burger et al. (1994) described three mannitol polymorphs melting at 158, 166 and 166.5 °C. Cavatur and Suryanarayanan (1998) reported that the melting point of β-mannitol was 165 °C. According to the results of this study, the pure mannitol does not change its crystal form in SEDS process but only decreases in crystallinity.

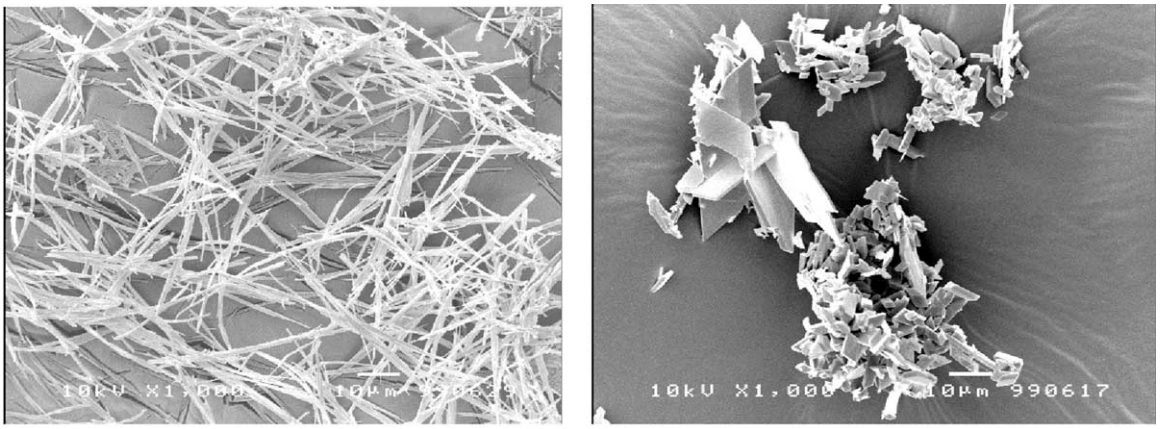

(a) (b)

Fig. 2. SEM graphs of (a) mannitol and (b) drug processed with SEDS using the same conditions as for the drug–mannitol mixtures. Scale bar represents 10 μm.

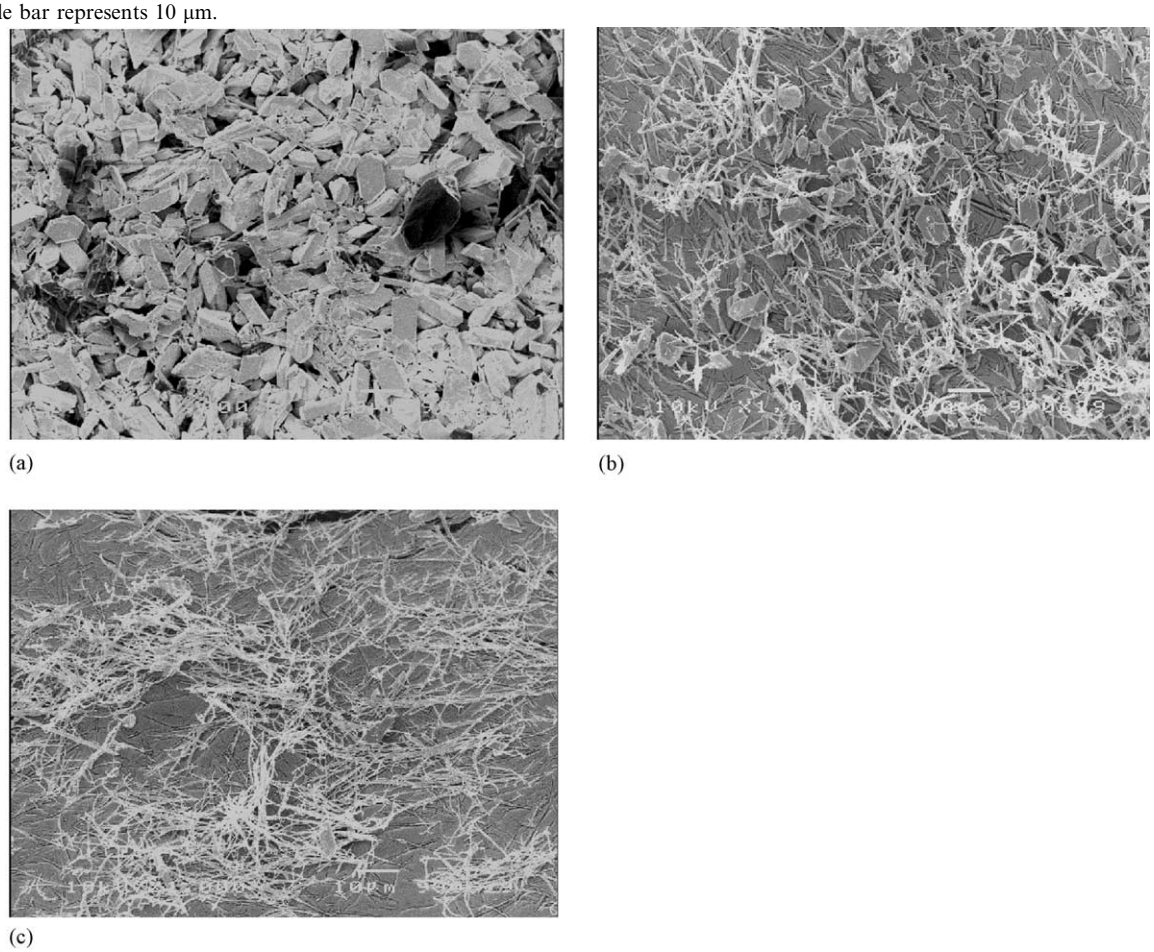

(a) (b)

(c)

Fig. 3. SEM graphs of drug–mannitol mixtures processed with SEDS. Drug–mannitol ratios: (a) 90:10, (b) 40:60, (c) 20:80. Scale bar represents 10 μm.

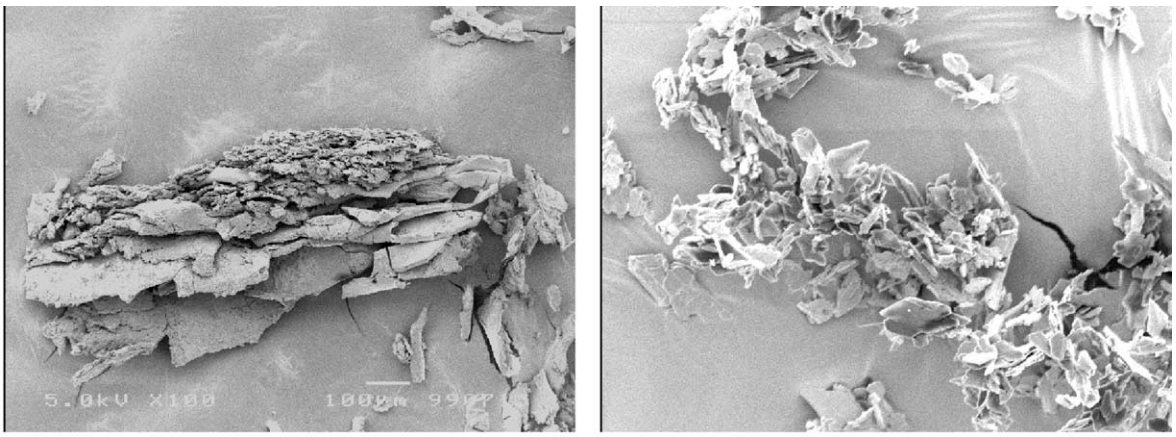

(a) (b)

Fig. 4. SEM graphs of (a) Eudragit® E100 and (b) drug processed with SEDS using the same conditions as for the drug–Eudragit® E100 mixtures. Scale bar represents 100 μm.

The pure drug behaves differently; both the melting temperature (205.8–210.3 °C) and the melting enthalpy (94.0–96.0 J/g) increased with the SEDS process (Fig. 6b). This may be explained by the drug substance achieving greater purity and higher crystallinity of drug substance when processed with supercritical fluids. This phenomenon is well known and has been utilised in purification of crystal materials (Shishikura et al., 1994). The supercritical fluids can extract impurities from the material. According to the pretests with the drug substance in SEDS process and with analysis with FT-Raman, the drug was proved to be precipitated as a mesylate salt.

3.3.2. Drug–mannitol

When the nominal drug content is 10%, no indication of crystalline drug can be detected in thermogram (Fig. 7a). The mannitol peak has shifted to lower temperatures (166.7 °C, 264.9 J/g) compared with the pure SEDS-processed mannitol, which is due to the drug behaving as an impurity in the system. When cooling, a recrystallisation exotherm is seen at 116.4 °C (−193.4 J/

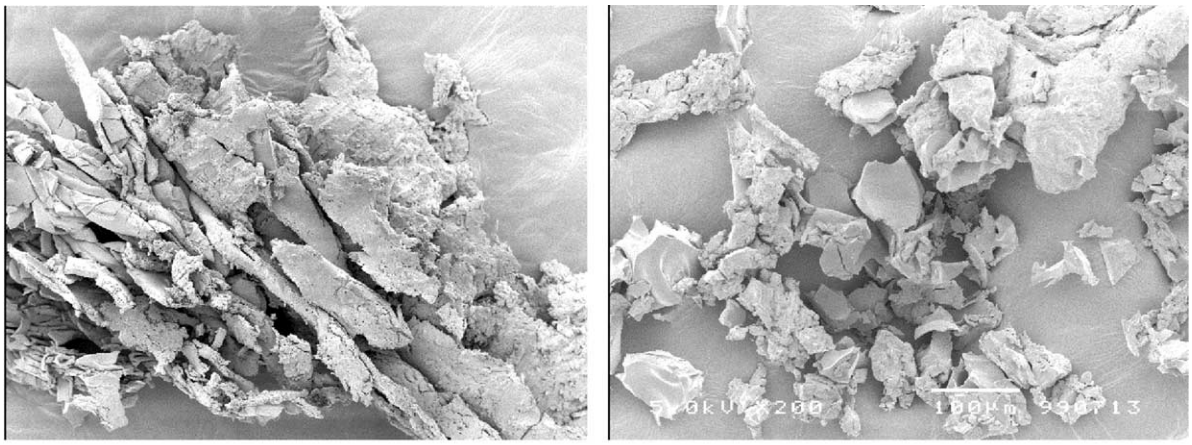

(a) (b)

Fig. 5. SEM graphs of drug–Eudragit® E100 mixtures processed with SEDS. Drug–Eudragit® E100 ratios: (a) 5:95, (b) 20:80. Scale bar represents 100 μm.

g) and as two other peaks at lower temperatures. When re-heating the sample, a melting peak of mannitol can be seen at 166.3 °C with a lower enthalpy, and there is a small peak at 155.5 °C (7.4 J/g) which might represent traces of another polymorph of mannitol. This recrystallisation phenomenon was not found with lower amounts of mannitol. Increasing the amount of drug to 20% resulted in the shift of the mannitol peak to 165.4 °C (248.6 J/g). The drug probably consists of predominantly amorphous material, since no drug melting peaks were observed.

The existence of drug peaks can first clearly be detected in the 50:50 mixture where it consists of two polymorphs, having melting points of 203.2 °C (called as form A or a partly eutectic mixture) and 210.2 °C (to be called as form B, 5.7 J/g, Fig. 7b). During cooling, the recrystallisation occurs at higher temperatures. It is possible that the form A or B recrystallises to a third form C (217.4 °C). Mannitol peak has shifted further downwards to 164.4 °C (194.8 J/g).

The recrystallisation of two forms during cooling is seen even in the 60:40 mixture and in the

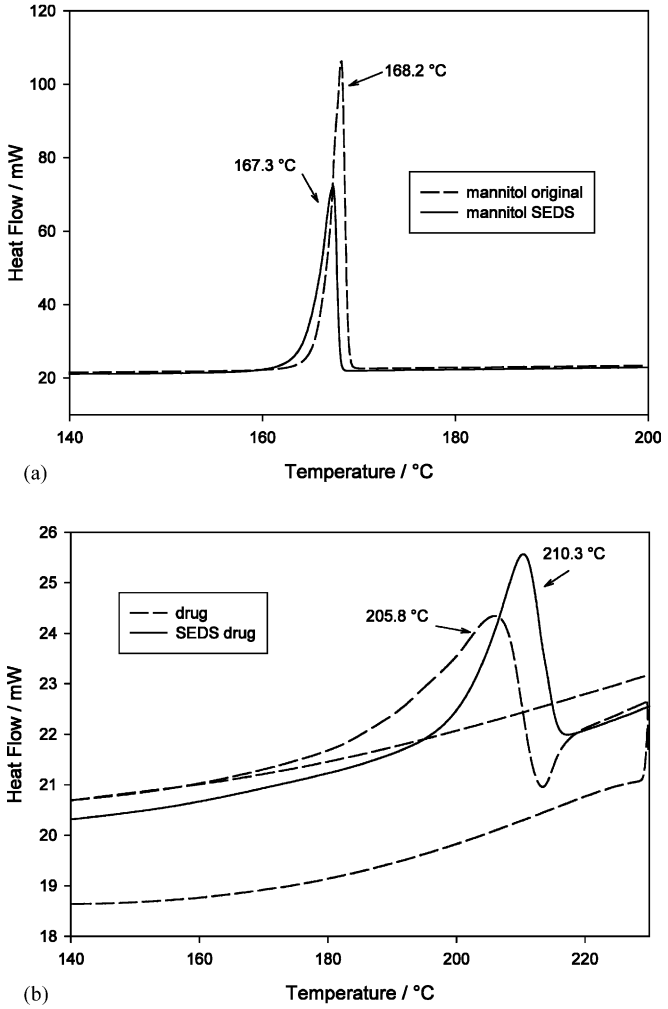

Fig. 6. Effect of SEDS processing on the DSC thermograms of (a) mannitol and (b) drug.

70:30 mixture, where the drug peak has shifted to 169.1 °C (Fig. 7c). During cooling the recrystallisation of form C may be observed as well as slight remelting of form A (or an eutectic mixture) at 194.7 °C (Fig. 7c). At such high amounts of drug, not only the crystal form of the drug but also that of mannitol is clearly affected. In addition to the main mannitol peak at 162 °C a new peak at 155.9 °C can be found. This could be due to melting point depression, or a sign of formation of

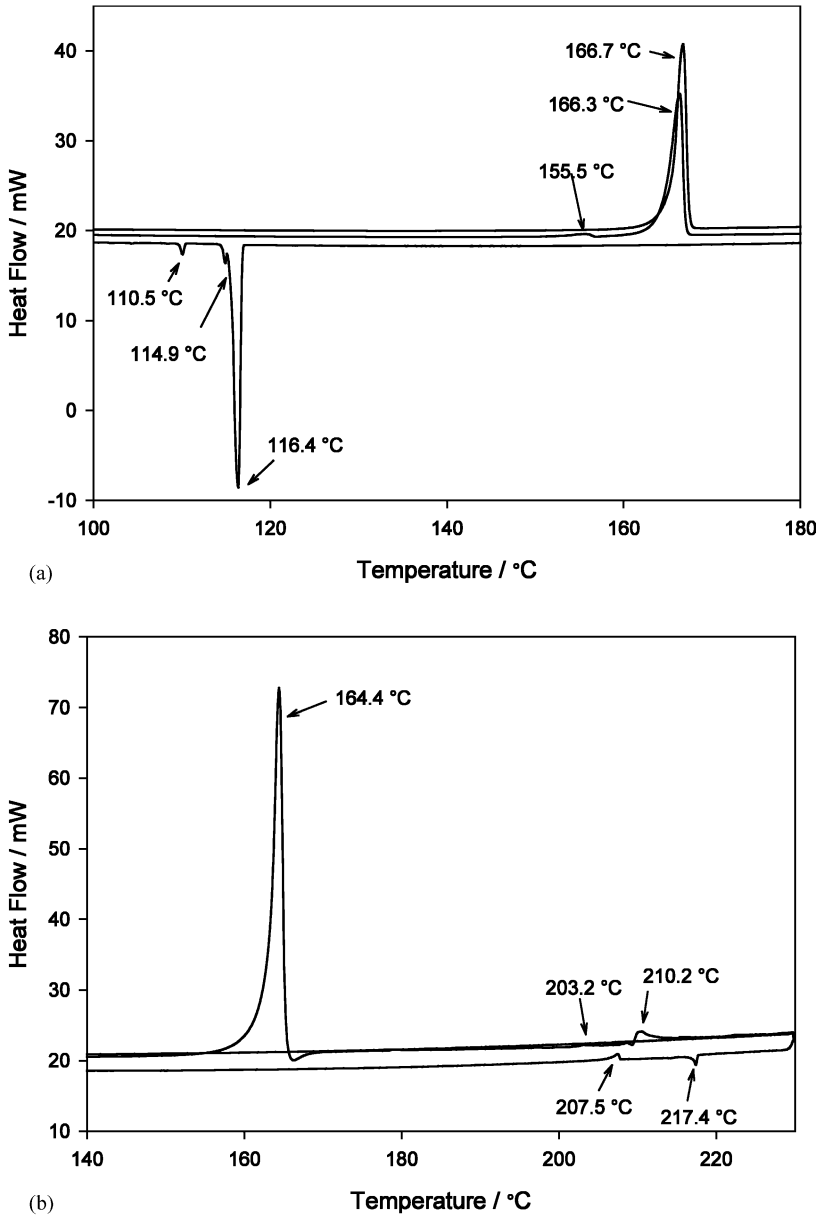

Fig. 7. DSC thermograms of drug–mannitol mixtures processed with SEDS. Drug–mannitol ratios: (a) 10:90, (b) 50:50, (c) 70:30.

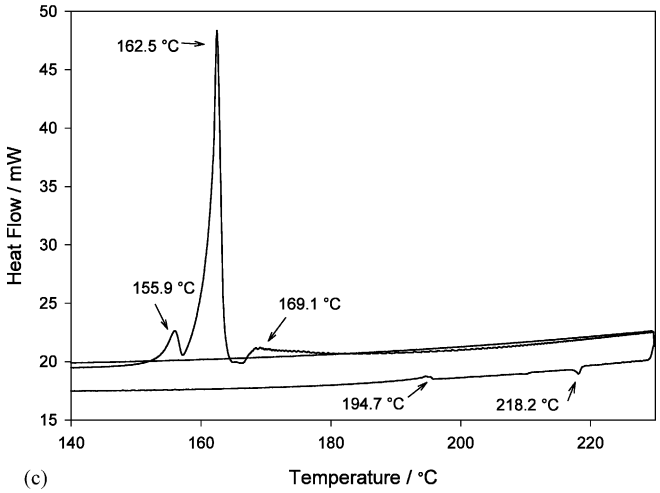

Fig. 7 (*Continued*)

the α-form. According to Burger et al. (1994), one of mannitol polymorphs had a melting point at 158 °C.

3.3.3. Drug–Eudragit® E100

No peaks were seen in thermograms of drug–Eudragit® E100 mixtures because both the drug and the excipient were amorphous. Thus, the polymer appears to be a good carrier for solid dispersions. Eudragit® E100 is known to suppress the recrystallisation in solid dispersion particles prepared by solution evaporation/milling (Moneghini et al., 1998) and by spray drying (Jung et al., 1999).

3.4. FTIR spectroscopy

3.4.1. Drug–mannitol

The spectra of the SEDS-processed mannitol and drug are shown in Fig. 8b and d, respectively. Tentative assignments are given in Table 3 (Colthup et al., 1975; Bellamy, 1975 and 1980).

The mannitol spectrum is dominated firstly by the strong primary alcohol OH stretching vibration showing peaks at 3392 and 3289 per cm. These OH groups in mannitol are hydrogen bonded to each other; free hydroxyl groups would manifest themselves at higher frequency at about 3600 per cm. At low frequencies, C–O stretching present in primary and secondary alcohols, respectively, 'R–CH_2–OH' and 'R–CHOH–R', dominates, and shows strong absorptions at 1082 and 1020 per cm.

The drug spectrum is dominated by the absorption bands 3389 and 3337 per cm at high frequencies, most probably attributable to N–H stretching of the secondary amine group positioned between the heterocyclic ring and the benzyl group, together with the O–H stretching of the primary alcohol (–CH_2–OH) group. At low frequencies, the bands between 1663 and 1423 per cm are attributed predominantly to C–N stretching and C–C ring stretching. The 1235, 1158, and 1039 per cm bands probably belong to the sulfonic acid salt functionality. Some of the absorption bands observed in the drug spectrum may be attributed to crystal packing/ordering and not to specific molecular group functionalities.

Changes arising from the SEDS process itself were also evaluated by comparing FTIR spectra of SEDS-processed drug with the unprocessed drug, and those of SEDS-processed mannitol with the unprocessed mannitol. Applying spectral subtraction procedures based on the internal absorbance band at 1588 per cm (C–C ring stretch), and 1320 per cm (OH deformation and CH_2 wag), for the drug and mannitol, respectively, the subtraction results (not shown here) indicated that no significant changes on a molecular level have occurred due to either the drug, or to mannitol, due to the

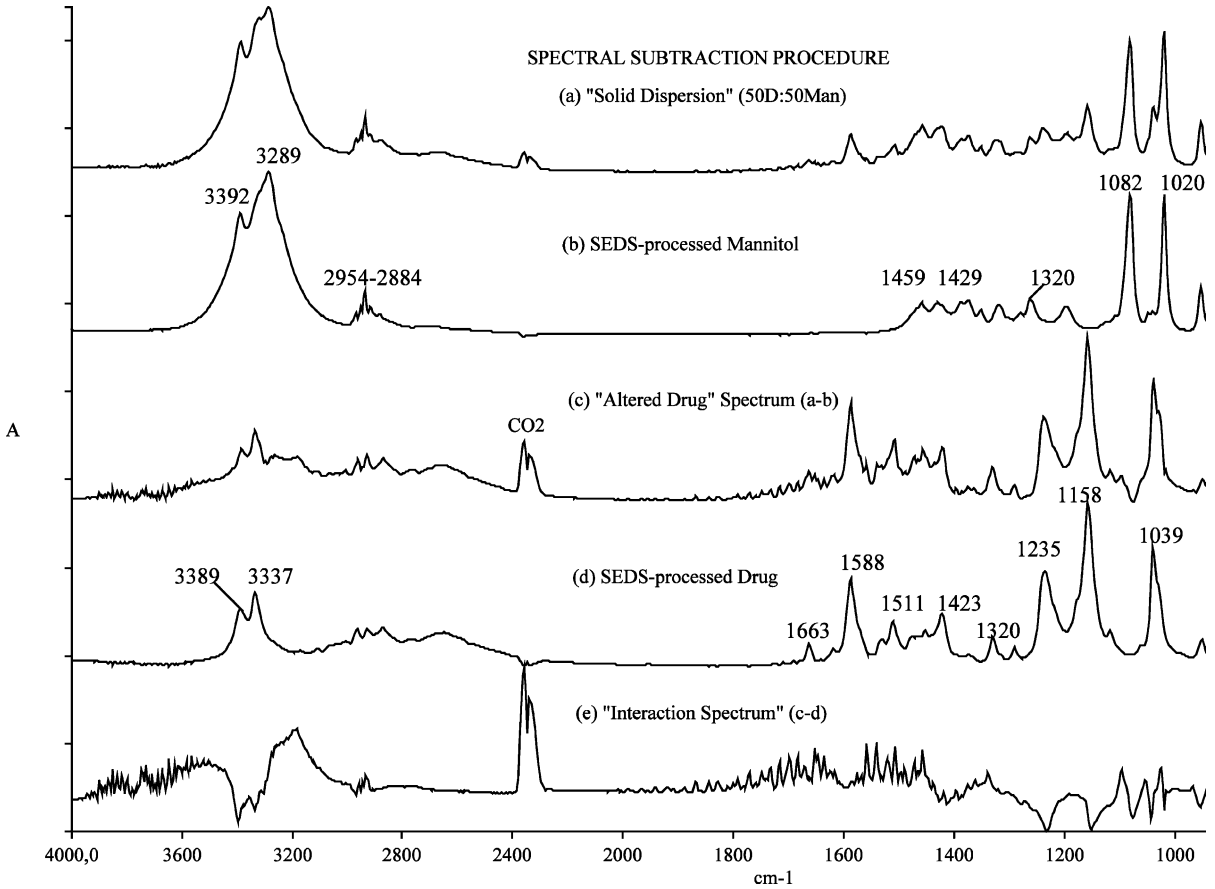

Fig. 8. FTIR spectra of (a) sample containing 50% drug, (b) SEDS-processed mannitol (control 1), (c) 'altered drug' (subtraction spectrum (a–b)), (d) SEDS-processed drug (control 2), (e) 'interaction spectrum' (subtraction spectrum (c–d)).

SEDS process, although some minor structural perturbations may have occurred. These results are in agreement with the DSC results discussed earlier.

Fig. 9 shows the spectra of the samples of drug and mannitol blends processed together using SEDS. The spectra represent, respectively, samples containing (a) 90%; (b) 70%; (c) 50%; (d) 30% and (e) 20%, of drug (nominal content). It may be observed that the spectra change from that resembling the drug to that resembling mannitol.

Fig. 8 illustrates the steps in the spectral subtraction procedure (Cole and Painter, 1977; Antoon et al., 1977; Koenig et al., 1977) used to elucidate the molecular changes in the blends after SEDS processing; in this case for the (50:50) sample. The routine involved first subtracting the SEDS-processed mannitol spectrum from the spectrum of the blend sample, giving a spectrum of the 'altered drug' (c). The ether band at 1082 per cm was used as the internal standard for the subtraction. Note that the 'altered drug' spectrum closely resembles the drug spectrum (d). In the second stage, the subtraction, (c)–(d) was performed, giving the 'interaction spectrum', which highlights the total changes occurring. The ring-stretching band at 1588 per cm was used as the internal standard for this subtraction.

Fig. 10 thus shows the interaction spectra for the (a) sample containing 90% drug (90D:10Man), (b) sample containing 50% drug (50D:50Man), (c) sample containing 20% drug (20D:80Man), and (d) physical mixture containing 70% drug (70D:30Man), for comparison. Note that these

Table 3
Assignments of the FTIR spectra

Frequency (per cm)	Assignment
(*1*) *Drug*	
3389	N–H stretching in the second amine group, attached to heterocyclic ring) and OH stretching
3337	N–H stretching in the second amine group, attached to heterocyclic ring)
2970–2820	Aromatic CH stretching
1663	C–N stretching in ϕ-C–N-ϕ
1588	C–C ring stretching
1511	C–N–H bending
1423	Ring stretching in trisubstituted benzene
1330	C–N stretching in aromatic amines
1291	C–N stretching in aromatic amines
1235	S–O stretching in sulfonic acid salt
1156	S–O stretching in sulfonic acid salt
1039	S–O stretching in sulfonic acid salt
(*2*) *Mannitol*	
3392	OH stretch
3289	OH stretch
2954–2884	CH_2 antisymmetric and symmetric stretch in CH_2–OH
1459	CH_2 deformation in CH_2OH
1429	OH deformation and CH_2 wag
1320	OH deformation and CH_2 wag
1082	C–O stretching in CH_2–OH
1020	C–O stretching and C–C–C stretching in R–CHOH–R
(*3*) *Eudragit® E100*	
2959–2900	Contributions from CH_3 antisymetric stretch, CH_2 antisymmetric stretching from CH_2–OR and CH_2 antisymmetric stretch from main chain
2823–2773	CH_2 symmetric stretch, from side chain CH_2–N–$(CH_3)_2$
1729	C=O stretch
1390	CH_3 stretch, possibly averaged between C–CH_3 (1378) and N–CH_3 (1410)
1148	Ester C–O stretch, next to C=O
1188	Ester C–O stretch
1462–1486	CH_2 deformation, from main chain

changes are very small, as observed from the small ΔA values (between 0.07 and 0.3). (Spectrum (a) is a little oversubtracted). In general, spectra (a)–(c) show similarities, especially in the low frequency region, where the derivative-appearing bands in each of these spectra, indicating small frequency shifts, lie at about the same frequencies. These shifts appear to be enhanced from (a) to (c), i.e. with increasing mannitol content, and indicate that more interactions occur when more mannitol is present. At the same time, some 'new' (positive) bands are clearly observed especially in spectra (b) and (c), at 3190, 1088 and 933 per cm. The first band at 3190 per cm, simultaneously observed with negative bands between 3340 and 3330 per cm, probably highlight the fact that the NH and OH functionalities have shifted to lower frequencies, due to hydrogen bonding, possibly between the NH or OH groups of the drug molecule and the OH groups of mannitol. The band at 1088 per cm probably indicates perturbations in the C–C–O vibrations of mannitol.

In the physical mixture, the interaction spectrum (d) appears somewhat different to the other three. The positive peak at 3190 per cm (together with the negative peak at about 3340 per cm) also indicates hydrogen bonding. However, the bands at 1418, 1282 and between 700 and 600 per cm show opposite subtraction results to those indicated in the other three interaction spectra. The bands between 1100 and 1000 per cm indicate perturbation in the C–C–O vibrations as before. There is thus a general indication of disturbance of both the drug and the mannitol structure, as well as some interaction, but the nature of both the interaction and perturbation is probably quite different to that obtained after SEDS processing.

Thus, the blending mannitol and the drug through the SEDS process, can lead to strong interactions, such as hydrogen bonding, as well as cause crystal changes/disruptions in both drug and excipient, leading to changes in relevant properties, such as solubility, as will be discussed later.

3.4.2. Drug–Eudragit® E100 system

Fig. 11 shows four spectra; (a) the SEDS-processed drug, (b) the sample containing 20% drug (20D:80Eu), (c) the sample containing 5% drug (5D:95Eu), (d) the SEDS-processed Eudragit® E100. Comparing firstly (a) and (d), it is observed that the drug and carrier spectra are very different.

The Eudragit® E100 spectrum is dominated by the carbonyl (C=O) stretching vibration at 1729

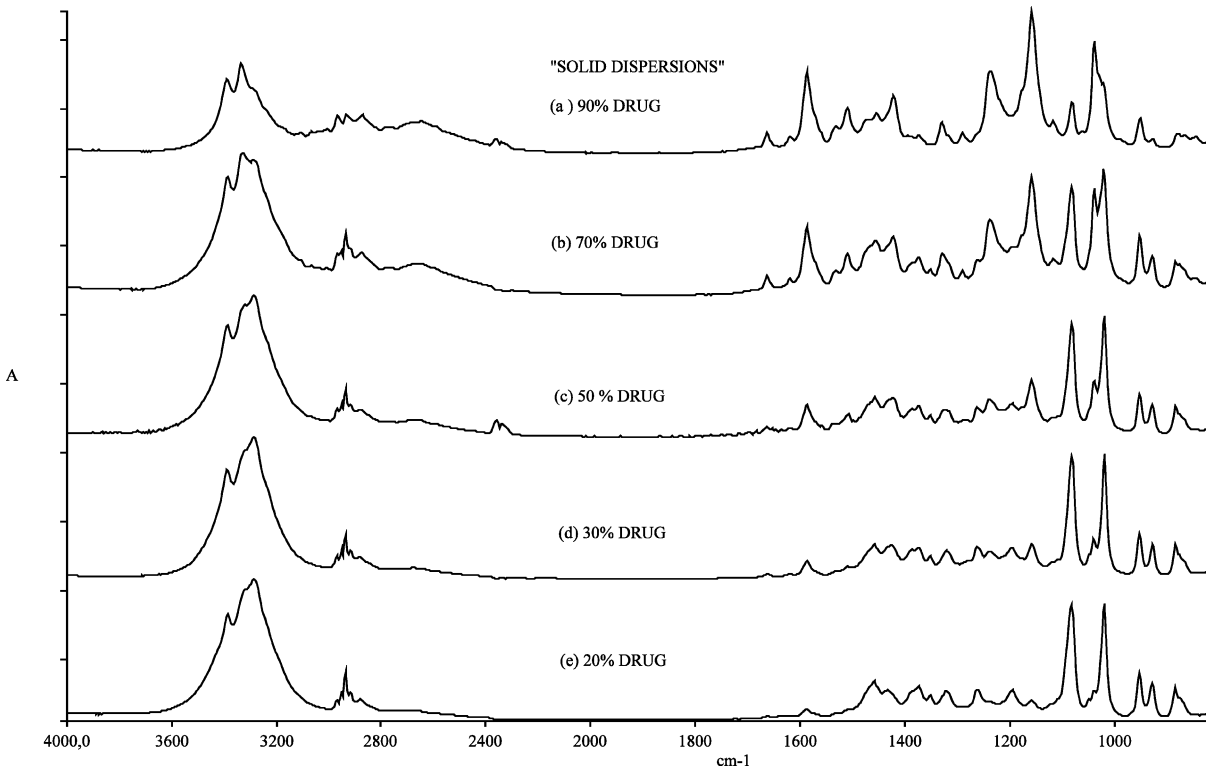

Fig. 9. FTIR spectra of samples containing (a) 90%, (b) 70%, (c) 50%, (d) 30%, (e) 20%, of drug (nominal content).

per cm as well as the ester C–O stretching vibrations at 1148 and 1188 per cm. Other assignments are given in Table 3. When the four spectra, (a)–(d) are compared, it is observed that both samples generated resemble the spectrum of Eudragit® E100.

Spectral subtraction was used as before to analyse these spectra more in detail, and the resulting interaction spectra (not shown here) were examined. It is observed that the main changes in the 20D:80Eu sample are positive interaction bands at 3485, 1711 (shifted to lower frequencies from 1729) per cm, indicating the appearance of hydrogen bonding interactions possibly between the acid OH group on the drug and the basic C=O group on the Eudragit® E100. The other main changes indicated by negative interaction drug bands suggest structural disturbances and possibly crystal changes in the drug molecule. However, in the 5D:95Eu sample, the presence of the band 3609 per cm indicates the presence of the free OH group, which suggests that less significant hydrogen bonding interactions have occurred here in this sample.

Thus, in this drug–Eudragit® E100 system, strong interactions can occur between Eudragit® E100 and the drug, leading to crystal changes/disruptions and the amorphous state, as observed with DSC, and quite likely, property changes like solubility. Unfortunately, this last conclusion could not be further substantiated with dissolution tests giving improved dissolution rate since the yields for this system in the SEDS process were so low that there was not enough material for dissolution tests.

3.5. Dissolution

The dissolution rate of drug–mannitol SEDS particles was higher than that of the SEDS-processed drug when the amount of drug was lower than 90% (Fig. 12). Most significantly, the samples, which did not give any drug peak in DSC analysis that is which appeared amorphous, re-

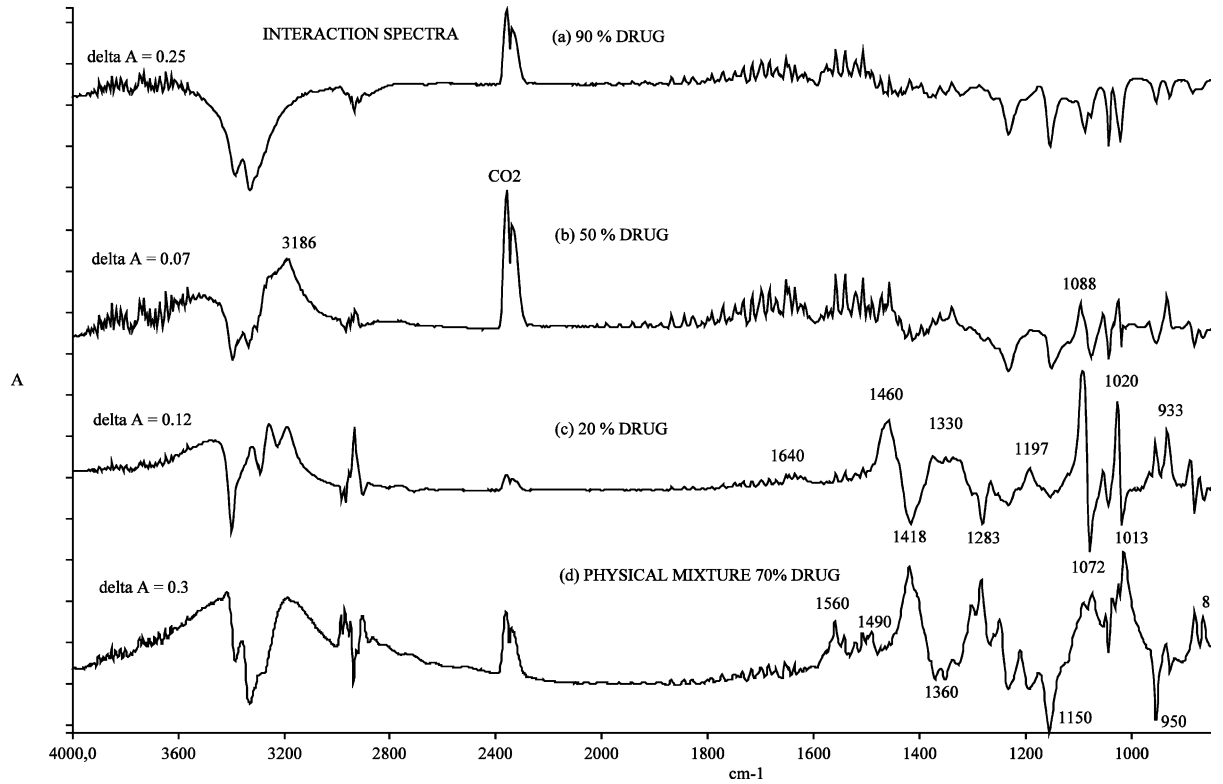

Fig. 10. Interaction spectra for the (a) sample containing 90% drug, (b) sample containing 50% drug, (c) sample containing 20% drug, (d) physical mixture, containing 70% drug.

leased the drug faster. Thus, interactions between the drug and mannitol and the changes in the drug crystal structure do appear to affect the drug release even if no real one-phase solid dispersion particles were formed. Unfortunately, no other certain conclusions can be made about the differences between the samples with different drug amounts due to the scarcity of samples tested (2 mg, $n = 2$). Further, the particle size of drug particles in the drug–mannitol mixtures could have some effect on the dissolution results even if no clear difference on particle size of different samples can be seen in the SEM graphs (Fig. 3).

4. Conclusions

It may be concluded that both drug and mannitol were affected by each other where crystal structure was concerned even if no true solid solution was obtained with this combination. The drug was not highly crystalline, since, only with 50% drug or higher, peaks in thermograms could be detected. The generally amorphous nature of the drug is a promising sign when considering solid dispersions and increase in solubility. Mannitol, used as a carrier, also decreased in crystallinity with increasing the amount of drug. Another polymorph of mannitol was formed when the amount of drug exceeded 70%. The strong interactions between the drug and mannitol could also be identified using FTIR as a hydrogen bonding between the amine or hydroxyl groups of the drug and the hydroxyl groups of mannitol. The changes in the crystal structure and the interactions caused by hydrophilic mannitol increased the dissolution rate of the drug even as the two-phase system.

However, a true solid solution was obtained when the drug was co-processed with Eudragit®

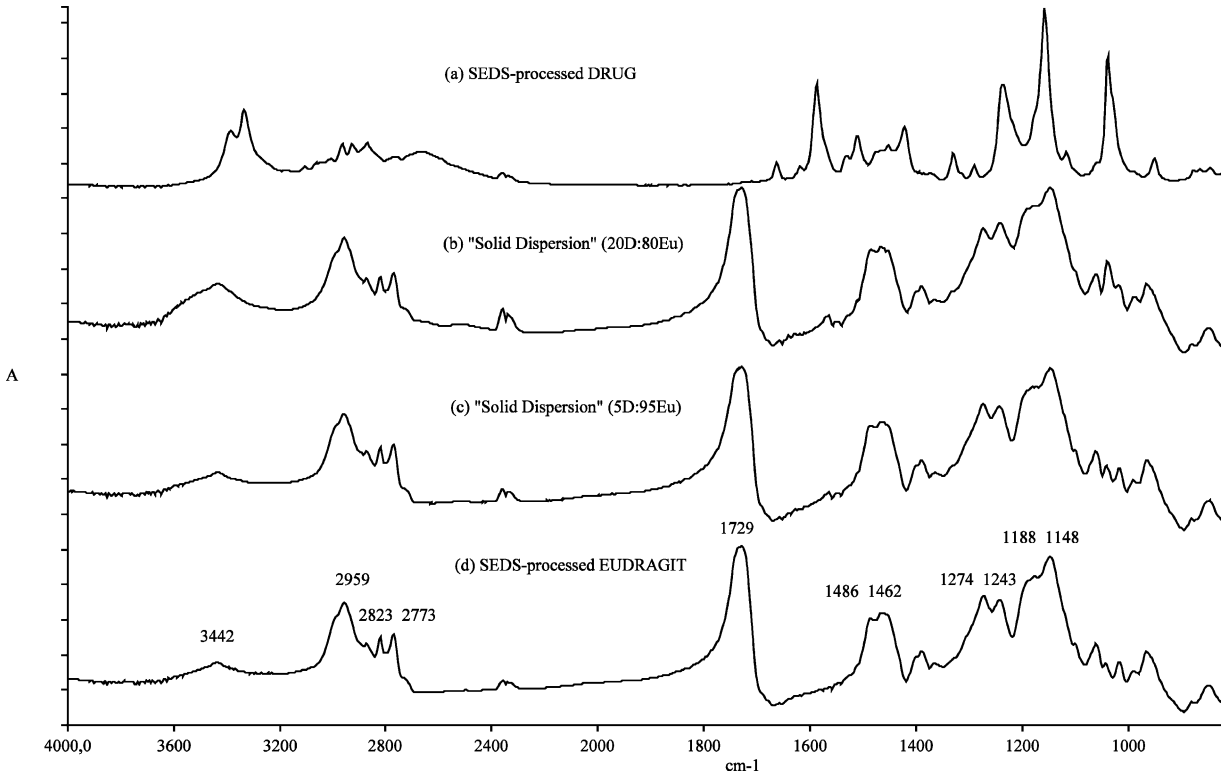

Fig. 11. FTIR spectra of (a) SEDS-processed drug, (b) sample containing 20% drug, (c) sample containing 5% drug, (d) SEDS-processed Eudragit® E100.

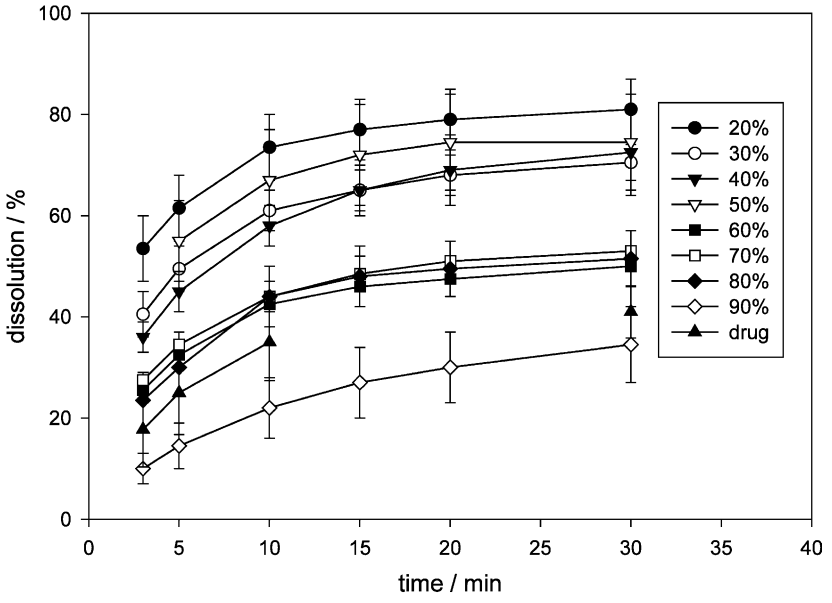

Fig. 12. Dissolution of drug–mannitol mixtures and pure drug processed with SEDS ($n = 2$). The error bar represents max and min.

E100, as expected. The blend particles resembled the SEDS processed polymer particles and no peaks were detected in the thermograms. The acid hydroxyl group of the drug showed a clear interaction with the basic carbonyl group on the Eudragit® E100. The disadvantage of this system processed in SEDS is that the polymer partly dissolved in the modified supercritical fluid due to its physicochemical properties. Thus, the yields of this system were very low. It is known that the polymers, which have a higher Tg and higher crystallinity, form more easily particles in supercritical fluid crystallisation (Bleich et al., 1993). Therefore, in order to get better yields, polymers with higher crystallinity, but with the same chemical functional groups, which are able to interact with the drug, should be chosen. A problem exists that the more crystalline polymers might dissolve too slowly. Another aspect is the chemical and physical stability of the solid solutions, which should be taken into account and investigated for the preferred formulation.

SEDS was shown to be an effective process for forming intimate blends and solid solutions for the drug with two different types of carriers. If the solid solutions are used to increase the dissolution rate of poorly soluble drug, the advantage of supercritical fluid processing is also its ability to form small particles with higher surface areas, which further increases the drug release rate. The formation of small particles is, however, highly dependent on the materials in question and requires optimisation of processing conditions.

Acknowledgements

We are grateful to Ylva Weimar and Carola Svanberg (AstraZeneca R&D Mölndal, Sweden) for their help with the dissolution tests and the drug content analysis. We are also grateful to Johanna Zandén for her help with the DSC analyses. Göran Wetter (Department of Electronics Packaging, Design and Production Research, The Swedish Institute of Production Engineering Research, Mölndal, Sweden) is thanked for his kind help with the EDS analyses.

References

Antoon, M.K., Koenig, J.H., Koenig, J.L., 1977. Least squares curve-fitting of Fourier transform infrared spectra with applications to polymer systems. Appl. Spectrosc. 31, 518–524.

Bauer, K.H., Lehmann, K.L., Osterwald, H.P., Rothgang, G., 1998. Coated Pharmaceutical Dosage Forms. CRC Press, Medpharm Scientific Publishers, Stuttgart.

Bellamy, L.J., 1975 and 1980. The Infrared Spectra of Complex Molecules. Vol. 1 and 2, Chapman Hall, London.

Bleich, J., Müller, B.W., Waßmus, W., 1993. Aerosol solvent extraction system—a new microparticle production technique. Int. J. Pharm. 97, 111–117.

Burger et al., 1994. Burger, A., Hetz, S., Weissnicht, A., 1994. On the polymorphism of mannitol. Eur. J. Pharm. Biopharm. 40 (suppl.), 21S.

Cavatur and Suryanarayanan, 1998. Cavatur, R.K., Suryanarayanan, R., 1998. Characterisation of phase transitions during freeze-drying by in situ x-ray powder diffractometry. Pharm. Dev. Technol. 3, 579–586.

Chiou, W., Riegelman, S., 1971. Pharmaceutical applications of solid dispersion systems. J. Pharm. Sci. 60, 1281–1302.

Cole, M.M., Painter, P.C., 1977. Fourier transform infrared studies of polymeric materials. J. Macromol. Sci. Rev. Macromol. Chem. C16, 197–313.

Colthup, N.B., Daly, L.H., Wiberley, S.E., 1975. Introduction to Infrared and Raman Spectroscopy, second ed. Academic Press, New York.

Dixon, D.J., Johnston, K.P., Bodmeier, R.A., 1993. Polymeric materials formed by precipitation with a compressed fluid antisolvent. Am. Inst. Chem. Eng. J. 39, 127–139.

Hanna, M., York, P., 1993. Method and apparatus for the formation of particles. Patent application WO9501221, 12 January.

Jung, J.-Y., Yoo, S.D., Lee, S.-H., Kim, K.-H., Yoon, D.-S., Lee, K.-H., 1999. Enhanced solubility and dissolution rate of itraconazole by a solid dispersion technique. Int. J. Pharm. 187, 209–218.

Koenig, J.L., D'Esposito, L., Antoon, M.K., 1977. The ration method for analyzing infrared spectra of mixtures. Appl. Spectrosc. 31, 292–295.

Krukonis, G., 1994. Gas antisolvent recrystallisation process. US patent 5, 360,478, 1 November.

Liu, G.-T., Nagahama, K., 1997. Solubility and RESS experiments of solid solution in supercritical carbon dioxide. J. Chem. Eng. Jpn. 30, 293–301.

Matson, D.W., Petersen, R.C., Smith, R.D., 1986. Formation of silica powders from the Rapid Expansion of Supercritical Solutions. Adv. Ceram. Mat. 1, 242–246.

Moneghini, M., Carcano, A., Zingone, G., Perissutti, B., 1998. Studies in dissolution enhancement of atenolol. Part I. Int. J. Pharm. 175, 177–183.

Müller, B.W., Fischer, W., 1989. Verfahren zur Herstellung einer mindestens einen Wirkstoff und einen Träger umfassenden Zubereitung. Patent application DE 3744329 A1, 6 July.

Senčar-Božič, P., Srčič, S., Knez, Ž., Kerč, J., 1997. Improvement of nifedipine dissolution characteristics using supercritical CO_2. Int. J. Pharm. 148, 123–130.

Serajuddin, A.T.M., 1999. Solid dispersion of poorly water-soluble drugs: early promises, subsequent problems, and recent breakthroughs. J. Pharm. Sci. 88, 1058–1066.

Schmitt, W.J., 1990. Finely divided solid crystalline powders via precipitation into an anti-solvent. Patent application WO90/03782 A2, 19 April.

Shieh, Y.-T., Su, J.-H., Manivannan, G., Lee, P.H.C., Sawan, S.P.S., Spall, W.D., 1996. Interaction of supercritical carbon dioxide with polymers. II. Amorphous polymers. J. Appl. Polym. Sci. 59, 707–717.

Shishikura, A., Kanamori, K., Takahashi, H., Kinbara, H., 1994. Separation and purification of organic acids by gas antisolvent crystallisation. J. Agric. Food Chem. 42, 1993–1997.

Tom, J.W., Debenedetti, P.G., 1991. Formation of bioerodible polymeric microspheres and microparticles by rapid expansion of supercritical solutions. Biotechnol. Prog. 7, 403–411.

Tom, J.W., Lim, G.-B., Debenedetti, P.G., Prud'homme, R.K., 1993. Applications of supercritical fluids in the controlled release of drugs. Proceedings from Supercritical Fluid Engineering Science American Chemical Society Symposium Series 514, pp. 238–257.

Ye, C., 2000. Enhanced dissolution of relatively insoluble drugs from small particles and solid dispersions formed from supercritical solutions. Ph.D. thesis, Ohio State University, USA.

Yeo, S., Debenedetti, P.G., Patro, S.Y., Przybycien, T.M., 1994. Secondary structure characterisation of microparticulate insulin powders. J. Pharm. Sci. 83, 1651–1656.

York, P., Wilkins, S.A., Storey, R.A., Walker, S.E., Harland, R.S., 2001. Coformulation methods and their products. Patent application WO 01/15664 A2, 8 March.